Characteristics of the carrier ground state of small semiconductor particles

1992 J. Phys.: Condens. Matter 4 L601

(http://iopscience.iop.org/0953-8984/4/44/002)

J. Phys.: Condens. Matter 4 (1992) L601–L606. Printed in the UK

LETTER TO THE EDITOR

Characteristics of the carrier ground state of small semiconductor particles

T Inaoka

Department of Materials Science and Technology, Faculty of Engineering, Iwate University, 4-3-5 Ueda, Morioka 020, Japan

Received 3 August 1992

Abstract. We investigate characteristics of the carrier ground state of small semiconductor particles by calculating the carrier density distribution and the effective one-particle potential self-consistently. We take account of the quantum mechanical boundary condition of semiconductor surfaces and the polarization of the dielectric background which accommodates carriers. In the case of n(p)-doping, the above boundary condition leads to a carrier-deficient surface layer with positive (negative) charges, and the inner surplus carriers operate to screen the positive (negative) charges in this surface layer, to build up the prominent peak in the carrier density profile. The effective potential bending downwards in the radial direction acts to lower the energy levels of carriers of larger angular momenta l.

Carrier states of semiconductor particles are significantly different from electronic states of metal particles in some points. For simplicity, we consider particles in the vacuum. For semiconductor particles, the kinetic energy of each carrier (tens of meV or less) is much smaller than the work function (several eV). Accordingly, the characteristic length of the carrier density variation near the surface is much longer than the penetration length of carriers into the vacuum. The former length is tens of Å or longer, while the latter length is one or a few Å. This situation is in sharp contrast with metal particles where the characteristic length of the electron density variation near the surface is comparable to the penetration length into the vacuum. (see e.g. figure 3 in [1]). The second point is that carriers are surrounded by the dielectric medium of the background. The polarization of this dielectric medium reduces the Coulomb interaction between carriers. In addition, when a carrier approaches some part of the particle surface, induced charges of the same sign occur at that part, owing to termination of the medium polarization at the surface. These induced surface charges act to repel the carrier into the inside of the particle. This effect is described by an image potential, as is shown below.

The aim of this brief report is to highlight characteristics of the carrier ground state of small semiconductor particles and to stress the difference from the electron ground state of metal particles. As a concrete object of study, we choose an n-doped GaAs particle which is spherical in shape. This particle can be considered to consist of the spherical dielectric and positive background carriers in it. The background polarization can be described by the static dielectric constant ϵ_0. The ionized donors in the background are assumed to be spread out into a uniform distribution of positive

0953-8984/92/440601+06$07.50

charges. In view of the quantum mechanical boundary condition of semiconductor surfaces, we assume that carriers are restrained in the particle by an infinite barrier potential at the surface of the particle, namely, that wave functions of carriers vanish at the surface. This assumption was employed to investigate the carrier-accumulation layer at the flat semiconductor surface [2] or at the flat oxide–semiconductor interface [3]. In n-doped compound semiconductors, such as n-GaAs, n-InSb and n-InAs, carrier electrons readily become degenerate with increase of carrier concentration, because combination of a very small effective electron mass and a large dielectric constant leads to a large effective Bohr radius a_B^*, and consequently, to a small effective carrier density parameter r_s. We are concerned with such highly degenerate carriers in the following calculation.

The ground state of carriers can be obtained by solving the following equations self-consistently:

$$\left\{-(\hbar^2/2m^*)\Delta + V_{\text{eff}}[r; n(r)]\right\}\psi_i(r) = E_i\psi_i(r) \tag{1}$$

$$n(r) = \sum_{i=1}^{N} |\psi_i(r)|^2 \tag{2}$$

where m^*, N, $n(r)$, $\psi_i(r)$, and E_i are the effective mass of carrier electrons, the number of carriers, the carrier number density at position r, the Kohn–Sham [4] single-particle eigenfunctions and eigenenergies, respectively. The effective one-particle potential V_{eff} is composed of the electrostatic Hartree potential V_H, the image potential V_{IM}, and the exchange–correlation potential V_{xc}. These potential components are explicitly written as

$$V_H[r; n(r)] = \frac{e^2}{\epsilon_0}\int d^3r' \frac{n(r') - n^+}{|r - r'|} \tag{3}$$

$$V_{IM}(r = \frac{\epsilon_0 - 1}{2\epsilon_0}\frac{e^2}{R}\sum_{k=1}^{\infty}\frac{k+1}{k\epsilon_0 + (k+1)}\left(\frac{r}{R}\right)^{2k} \tag{4}$$

$$V_{xc}[n(r)] = -\frac{e^2}{2\epsilon_0 a_B^*}\frac{2}{\pi}\left(\frac{9\pi}{4}\right)^{1/3}\left(\frac{1}{r_s(r)} + 0.0545\ \ln\left(1 + \frac{11.4}{r_s(r)}\right)\right). \tag{5}$$

In equations (3)–(5), R, ϵ_0, and n^+ denote the radius of the spherical particle, the static dielectric constant of the background, and the homogeneously smeared-out density of ionized donors, respectively. We adopt the spherical polar coordinates and locate the origin at the centre of the particle. The effective Bohr radius a_B^* and the local effective density parameter $r_s(r)$ are defined by $a_B^* = \epsilon_0\hbar^2/m^*e^2$ and $a_B^* r_s(r) = [3/4\pi n(r)]^{1/3}$, respectively. For the exchange–correlation potential, we invoke the local density approximation and employ the expression which was parametrized by Gunnarsson and Lundqvist [5].

We present the result of a self-consistent calculation for an n-doped GaAs neutral particle with $N = 92$ and $R/a_B^* = 3.463$ ($R = 352.8$ Å). This doping corresponds to the bulk carrier concentration $n_B = 5\times10^{17}$ cm^{-3}, namely, to the effective carrier density parameter $r_s = 0.7671$. The carriers have closed-shell configurations, which leads to the spherical symmetry of n and V_{eff}. The parameter values used in our

calculation are the static dielectric constant $\epsilon_0 = 12.9$ and the effective electron mass ratio $m^*/m_e = 0.067$.

Before analysing our result, we give explanations of figures 1 and 2. Figure 1 exhibits the r-dependence of the carrier number density n (the solid curve in (a)) and the effective one-particle potential V_{eff} (the solid curve in (b)). The carrier density n and the potential V_{eff} are scaled in units of $(a_B^*)^{-3}$ and $e^2/2\epsilon_0 a_B^*$, respectively ($a_B^* = 101.9$ Å and $e^2/2\epsilon_0 a_B^* = 5.478$ meV). The value of V_{eff} at the centre $r = 0$ is taken to be the energy origin. In panel (a), the dotted curves s, p, $\cdots$, h represent decomposition of n into components of various angular momenta l, and the upper dotted curve SW displays the density distribution of the carriers confined in a square-well potential $V(r) = 0$ for $r < R$ and ∞ for $r > R$. The broken line denotes the density of the homogeneously spread-out ionized donors. In panel (b), the horizontal bars indicate the occupied energy levels of the carriers, and the dotted curve represents the self-consistent effective potential in the Hartree approximation and in the absence of the image potential. Each energy level of angular momentum l in panel (b) is composed of $2(2l + 1)$-fold degenerate states, which are all occupied because 92 carriers take closed-shell configurations. For comparison with electronic states of metal particles, figure 2 shows the electron density profile, the effective potential, and the occupied electron energy levels of the metal particle with the electron number $N = 92$ and the effective electron density parameter $r_s = 4$. This result was obtained by Ekardt by virtue of combination of the spherical jellium background model and the local density functional approximation [1].

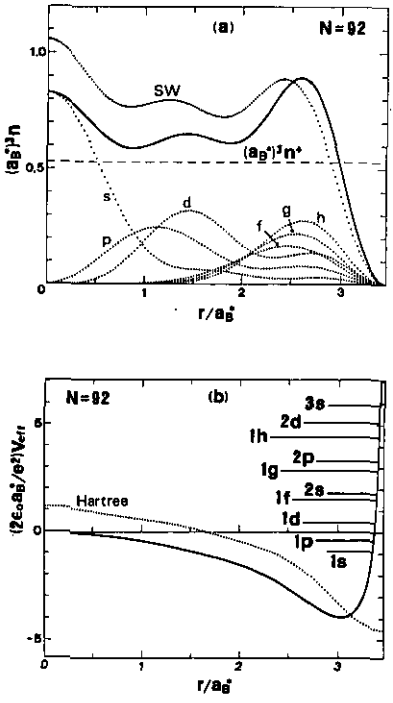

Figure 1. (a) The carrier density distribution and its decomposition into components of various angular momenta l. (b) The effective one-particle potential and the occupied energy levels of the carriers.

First, we focus our attention on the carrier density profile (see the solid curve in figure 1(a)). Pronounced oscillations result from standing waves which occur within the sphere. The most striking feature is the prominent peak near the surface. The peak around the centre of the particle stems only from the s states (1s, 2s and 3s). The value of the wave function falls and vanishes at the surface, which gives rise to a carrier-deficient surface layer with positive charges ($r/a_B^* \gtrsim 3$). The density distribution of carriers confined in a square-well potential (the dotted curve SW in figure 1(a)) shows that there is a great surplus of negative carrier charges inside the carrier-deficient surface layer. This excess of negative charges cancels with the positive charges in the surface layer to retain charge neutrality as a whole. This density distribution produces an effective potential which bends downwards to quite a low value with increasing r. This is, of course, not a self-consistent solution. To reach self-consistency, a considerable fraction of interior excess carriers must shift into the surface region, as is seen from comparison between the solid and dotted (SW) curves in figure 1(a). This asserts that internal excess carriers operate to screen the positive charges in the surface layer, to form the prominent peak close to the surface. The magnitude of this peak is considerably larger than the density of uniformly smeared-out positive donors. Carrier states of larger angular momenta l make a larger contribution to this peak. As is shown in figure 2 of [6], in metal particles, electronic states of larger l penetrate further into the vacuum, which suppresses the magnitude of the outermost peak in the electron density profile.

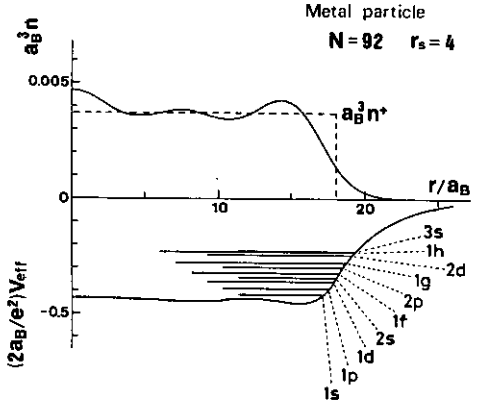

Figure 2. The electron density profile, the effective one-particle potential, and the occupied electron energy levels of the metal particle with 92 electrons. The broken line represents the jellium background of homogeneously smeared-out ions. a_B denotes the Bohr radius. Adapted from figure 3(i) in [1].

Next, we turn our attention to the effective one-particle potential V_{eff}. The r-dependence of V_{eff} is characterized by the downward bending and the steep ascent right in the neighbourhood of the surface. The downward bending arises from the inner negative charges due to excessive carriers and the surrounding positive charges in the carrier-deficient layer. This potential bending is in sharp contrast with the nearly flat r-dependence of V_{eff} inside the metal particle (see figure 2). The steep ascent originates from the effect of the image potential. This repulsive effect acts right in the vicinity of the surface. The occupied energy levels of carriers are identified as

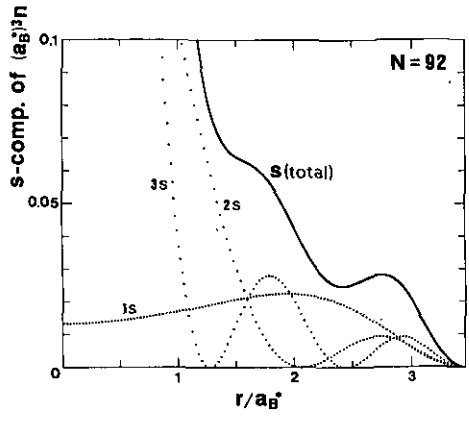

Figure 3. Decomposition of the s component of the carrier density distribution into three contributions of 1s, 2s and 3s. The dotted curves 2s and 3s have maximum values of $\simeq 0.21$ and $\simeq 0.61$ respectively, at the centre of the particle.

1s, 1p, 1d, 1f, 2s, 1g, 2p, 1h, 2d, and 3s in order of increasing energy (the horizontal bars in figure 1(b)). This energy-level series is significantly different from that for the metal particle. In the metal particle, the 1f, 1g, and 1h levels, which have larger l, lie above the 2s, 2p, and 2d levels, respectively (see figure 2). The reason why the energy levels of larger l tend to be lowered in the semiconductor particle is that the effective potential bends downwards to form a potential hollow, where the carrier states of larger l have their substantial probability density. The carrier states of larger l have higher centrifugal potential energies, which lead to positive values of energy levels in spite of localization into the potential hollow. The self-consistent effective potential in the Hartree approximation and in the absence of the image potential (the dotted curve in figure 1(b)) gives a good description of the downward bending. Because of absence of the exchange–correlation effect, this potential curve lies above the solid curve of the full calculation except in the vicinity of the surface. In the case of the flat neutral surface, the downward bending of the effective potential for the corresponding carrier concentration is evaluated to be $\simeq 3.8$ in units of $e^2/2\epsilon_0 a_B^*$, by means of a parametric Hartree calculation which takes no account of the image potential (see figure 5 in [2]).

The s component of n in figure 1(a) consists of three contributions of 1s, 2s, and 3s. This decomposition is displayed in figure 3. As is implied by its negative energy level, the 1s state shows signs of localization into the potential hollow, though it has appreciable probability density also around the centre of the particle.

I would like to express my thanks to Professor M Hasegawa for valuable discussions. I am grateful to Professor M Watabe for useful comments. This work is supported by a Grant-in-Aid for Scientific Research from the Ministry of Education, Science and Culture, under No 04640359.

References

[1] Ekardt W 1984 *Phys. Rev.* B **29** 1558

[2] Baraff G A and Appelbaum J A 1972 *Phys. Rev.* B **5** 475
[3] Ando T 1975 *J. Phys. Soc. Japan* **39** 411
[4] Kohn W and Sham L J 1965 *Phys. Rev.* **140** A1133
[5] Gunnarsson O and Lundqvist B I 1976 *Phys. Rev.* B **13** 4274
[6] Puska M J, Nieminen R M and Manninen M 1985 *Phys. Rev.* B **31** 3486